Solvent Effects on the Binding of Fatty Acids to Human Serum Albumin

P. Pant, Y. B. Ruiz-Blanco, E. Sanchez-Garcia

published in

NIC Symposium 2020
M. Müller, K. Binder, A. Trautmann (Editors)

Forschungszentrum Jülich GmbH,
John von Neumann Institute for Computing (NIC),
Schriften des Forschungszentrums Jülich, NIC Series, Vol. 50,
ISBN 978-3-95806-443-0, pp. 147.
http://hdl.handle.net/2128/24435

Solvent Effects on the Binding of Fatty Acids to Human Serum Albumin

Pradeep Pant, Yasser B. Ruiz-Blanco, and Elsa Sanchez-Garcia

Computational Biochemistry, Center of Medical Biotechnology,
University of Duisburg-Essen, 45117 Essen, Germany
E-mail: elsa.sanchez-garcia@uni-due.de

Solvent interactions can influence the properties and function of complex biomolecules. Among others, altering the solvent composition has consequences for the recognition of binding partners. Human serum albumin (HSA) is one of the most enigmatic biomolecules, known as an efficient carrier of biological materials, such as hormones, fatty acids and drugs.

Here we explored the effects of the solvent on stearic acid-HSA binding. To this end, we performed all-atom molecular dynamics (MD) simulations in explicit solvent ($\sim$ 2.9 µs in total). These MD simulations were carried out in explicit water and in a 20 % ethanol-water mixture. The sampling in both systems was processed with the MM-PBSA binding free energy approach, which allowed us to investigate the effects of the solvent composition on the binding of stearic acid molecules to seven binding sites of HSA. Using this computational approach, we were able to reproduce the experimental preference of fatty acid's binding sites for albumin in water. **Site 5** $>$ **site 4** $>$ **site 2** were calculated as high affinity fatty acid binding sites, in agreement with the experimental reports.[1] Interestingly, we observed that **site 1** becomes the most prominent binding pocket in the 20 % ethanol-water mixture, with overall binding affinity towards stearic acid: **site 1** $>$ **site 5** $>$ **site 2.** Our simulations in explicit solvent also provided a rationale for this effect. Importantly, we achieved weak binding-to strong binding conversion by using a solvent mixture, with repercussions for the specific binding properties and the manipulation of HSA properties as biological carrier.

1 Introduction

Human serum albumin (HSA) is a 585 residues protein found in most fluids of the body.[2–4] HSA acts as depot and carrier for a broad spectrum of compounds like fatty acids and affects the pharmacokinetics of many drugs such as penicillin and sulphonamides.[5, 6] HSA also acts as a toxic waste handler.[7] Furthermore, HSA displays pseudo enzymatic properties and it is a valuable biomarker in many diseases.[8, 9] HSA features several binding sites for medium to long chain fatty acids, wherein lauric acid (C12), myristic acid (C14), palmitic acid (C16), and stearic acid (C18) are commonly found.[10]

Changes in solvent media[11–13]can strongly affect molecular interactions that occur routinely in aqueous solution. Protein-protein, protein-DNA, and protein-RNA recognition are progressed by water-mediated hydrogen bonds.[14–16] Thus, the hydrogen bond donor and acceptor capabilities of water often play a crucial role in biological recognition.[17–19] Solvent mixtures have been extensively used to unravel macromolecular and recognition events such as protein binding hotspots identification, ligand binding, protein folding, and the elucidation of biological mechanisms.[13, 20–22] HSA in particular displays three high-affinity fatty acid binding sites and four weakly binding sites in water, which were confirmed by several experimental and theoretical studies.[23–25] However, to the best of our knowledge, the solvent-driven regulation of stearic acid binding to albumin has not been addressed.

Here, we explored the binding of stearic acid to HSA (Fig. 1) in water and in a 20 % ethanol-water mixture. The simulations in water were used as reference and control system. There, we were able to reproduce the experimental order of binding of stearic acid to the seven binding pockets of HSA, validating our computational protocol. A different binding site (**site 1**) emerged as preferred in the 20 % ethanol-water mixture. This can be explained by an enhanced hydrogen bond network between stearic acid and HSA in **site 1**, involving nearby ethanol molecules. Energy calculations using the MM-PBSA[26] approach also indicated enhanced electrostatics effects in the ethanol-water system.

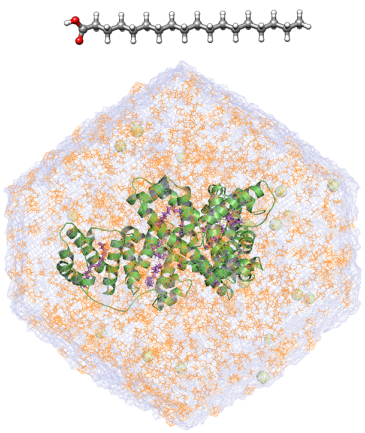

Figure 1. Top: Stearic acid (C18), carbon atoms are shown in grey, oxygen in red, hydrogen in white. Bottom: Representative structure of HSA in 20 % ethanol-water, water is shown as a blue mesh surface, ethanol molecules in orange, stearic acid in violet and ions as green spheres.

2 Methods

A crystal structure of human serum albumin (RCSB PDB:[27] 1E7I, resolution: 2.7 Å) was taken as starting structure for the computational studies. The first two N-terminal residues (aspartic acid, alanine) and the C-terminal leucine were missing in the crystal structure and hence were subsequently modelled by us using I-Tasser.[28] The Root Mean Square Deviation (RMSD) differences between the energy minimised structure and the crystal structure was 0.2 Å. The available crystallographic data of palmitic acid in HSA[29] (PDB ID: 4BKE) was used to set the initial orientations of the stearic acid in HSA since, in the 1E7I complex, some of the fatty acid molecules missed the carboxyl group. The protonation states of the titrable residues of HSA were determined using the H++ server[30] and corroborated by visual inspection. MD simulations were performed using the AMBER 14[31] and NAMD 2.12b software suites.[32] An octahedral water box of 15 Å was generated as both reference and control system along with the requisite counter ions to neutralise the system. The modified ff99SB force field[33] was used for the protein in the simulations with AMBER 14, and the CHARMM36m force field[34] was used in the simulations with

NAMD 2.12b. Stearic acid parameters for AMBER were generated at the HF/6-31G*[35] level of theory using Gaussian09.[36, 37] PME was used to treat long-range electrostatic interactions.[38] The system was first minimised (15 000 CG + 15 000 SD) and then equilibrated for 5 ns (at room temperature) followed by 50 ns of production run to allow the structure to relax in the aqueous environment. The last frame comprising HSA with seven stearic acid molecules in their binding pockets was used to generate seven starting systems (HSA with only one ligand). Each of those systems was again simulated (3 independent replicas of 50 ns each). The MM-PBSA approach was used for computing the binding free energies. The Cpptraj[39] module of AMBER was utilised for the analysis of the MD trajectories (RMSD fluctuations, hydrogen bonding). The 20 % ethanol-water mixture was generated using Packmol,[40] a freely accessible tool that creates initial configurations for MD simulations. For HSA in the 20 % ethanol-water mixture, we followed a protocol analogous to that described for HSA in water. The equilibrated structure of albumin in the 20 % ethanol-water mixture is shown in Fig. 1.

3 Results and Discussion

The molecular dynamics simulation trajectories were visualised using the VMD tool.[41] HSA with seven stearic acid molecules occupying simultaneously all the possible binding sites was first simulated for 50 ns in an octahedral box with counterions added to neutralise the whole system. The backbone RMSD fluctuations throughout the trajectory were below 3.0 Å indicating no overall large dynamical changes in the structure. The final frame of this trajectory was used to generate seven initial systems, with a single stearic acid molecule in each of the seven binding pockets of HSA. These systems were further relaxed by performing 50 ns long MD simulations as per the protocol discussed in the Methods section. We observed stable control plots of temperature, pressure, density and total energy (kinetic and potential) along with low RMSD fluctuations. The last frame of this MD provided the initial coordinates for performing three replicas of 50 ns of each system.

From the sampling in water, we extracted 500 frames, which were used to calculate the binding free energies of stearic acid in the fatty acid-binding sites of HSA using the MM-PBSA approach, which has been extensively applied to estimate binding free energies of small molecules in the binding pocket of macromolecular systems[25] (Tab. 1). We observed that in water, **site 5** has the highest binding affinity for stearic acid (-24.5 $\pm$ 0.59 kcal/mol (Tab. 1)), followed by **site 4** (-18.96 $\pm$ 0.76 kcal/mol) and **site 2** (-18.15 $\pm$ 0.82 kcal/mol). These three regions are also reported as high affinity fatty acid-binding sites in the literature.[1] Other binding spots, classified as low affinity, have binding energies $>$ -15 kcal/mol, also in agreement with experimental observations[24, 25] and validating our protocol of simulations and energy estimations using MM-PBSA. We note that the change in the dielectric constant of the system from water to the 20 % ethanol-water mixture is not expected to affect significantly the evaluation of the Poisson's equation for continuum electrostatics. Also, the contributions of non-polar groups (which is proportional to the variation of the solvent accessible surface area) is expected to be lower than for more polar systems like pure water. Hence the MM-PBSA approach for calculating binding free energy remains a suitable protocol in water-organic solvent mixtures at moderate or low organic solvent fraction.

Binding sites	Water	20 % ethanol-water
Site1	-13.6 (0.93)	-29.9 (0.81)
Site2	-18.2 (0.82)	-23.9 (0.81)
Site3	-6.5 (0.84)	-6.2 (0.57)
Site4	-19.0 (0.76)	-13 (1.71)
Site5	-24.5 (0.59)	-24.0 (0.62)
Site6	-12 (1.02)	-16 (1.01)
Site7	-14.8 (0.68)	-12 (1.09)

Table 1. Energetics of binding of stearic acid molecules (in kcal/mol) in the seven fatty acid binding sites of HSA in water and in the 20 % ethanol-water mixture. SE of mean indicated in parentheses.

Further, we examined the binding proclivity of stearic acid in the binding pockets of HSA in the 20 % ethanol-water system. **Site 1** emerged as the preferred spot with the most favourable binding free energy for stearic acid (-29.88 $\pm$ 0.81 kcal/mol) followed by **site 5** (-24.01 $\pm$ 0.62 kcal/mol) and **site 2** (-23.89 $\pm$ 0.81 kcal/mol). These results evidence how altering solvent composition induces a low-binding to high binding transition and overall enhances the binding affinity of stearic acid towards HSA.

The analysis of the contributions to the free energy of binding of stearic acid in **site 1** (Fig. 2) indicates a remarkable increment in the total electrostatic contribution in the 20 % ethanol-water mixture with respect to water, leading to an enhanced binding of stearic acid to HSA in ethanol-water.

The 2-D interaction diagrams (plotted using the LigPlot+ software[42]) allowed us to rationalise the enhanced electrostatics contributions of stearic acid in **site 1** of HSA in the

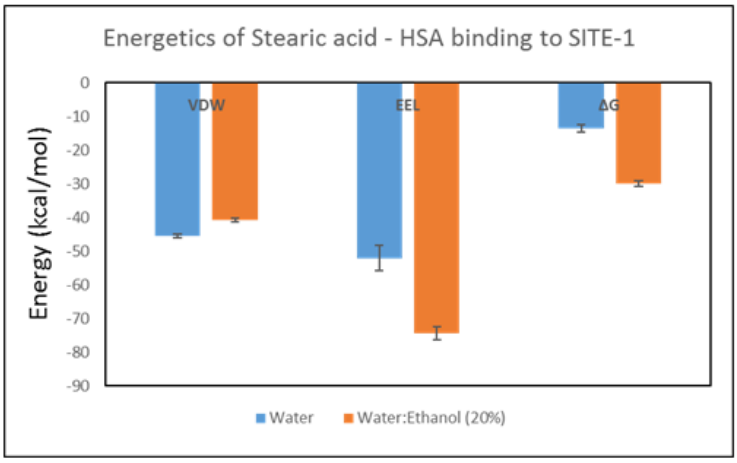

Figure 2. Electrostatic and van der Waals contributions to the total free energy of binding for the stearic acid (**site 1**)-HSA system in water (blue) and in the 20 % ethanol-water mixture.

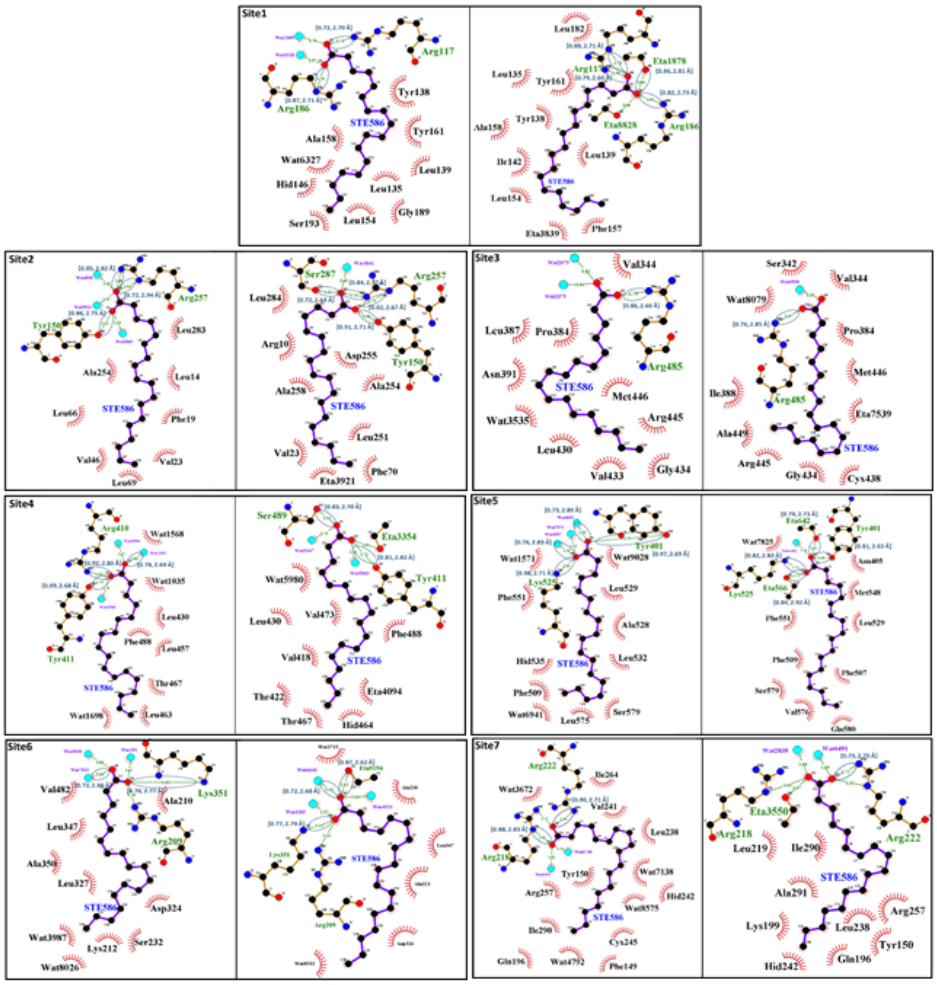

Figure 3. 2-D interaction plots of stearic acid in the seven fatty acid binding pockets of human serum albumin. All hydrogen bonds with lifetime > 0.70 are highlighted. In all cases, the left panel corresponds to the simulations in water and the right panel to the simulations in the 20 % ethanol-water mixture. The lifetime fraction of these hydrogen bonds and the average h-bond distances are shown in parenthesis (format: [lifetime fraction, average distance], see Tab. 2).

ethanol-water mixture (Fig. 3, hydrogen bond interactions with a fraction half-life time larger than 0.70 are highlighted). In water environment, stearic acid establishes in **site 1** two conserved hydrogen bonds with HSA residues (Arg 117 and Arg 186). However, in the 20 % ethanol-water mixtures, the stearic acid molecule in **site 1** is able to establish four conserved hydrogen bonds (Arg 117, Arg 186 and two ethanol molecules) (Tab. 2).

On the other hand, **site 4** shifts from a high affinity site to a low affinity site upon addition of methanol to the water solvent environment. The analysis of the interactions in this site allows us to rationalise this observation (Fig. 3). In water, stearic acid displays

	Water			20 % ethanol-water		
Binding site	Residue	Average h-bond distance (Å)	Fraction of h-bond lifetime	Residue	Average h-bond distance (Å)	Fraction of h-bond lifetime
Site1	Arg186	2.71	0.87	Arg186	2.73	0.82
	Arg117	2.70	0.72	Arg117	2.60	0.79
				Arg117	2.71	0.88
				ETA	2.81	0.86
Site2	Arg257	2.94	0.72	Arg257	2.67	0.82
	Arg257	2.82	0.85	Arg257	2.77	0.84
	Tyr150	2.75	0.86	Tyr150	2.67	0.82
				Ser287	2.64	0.72
Site4	Tyr411	2.68	0.89	Tyr411	2.82	0.81
	Arg410	2.80	0.92	Ser489	2.70	0.83
	WAT	2.69	0.79			
Site5	Tyr401	2.69	0.92	Tyr401	2.63	0.81
	Lys525	2.71	0.98	Lys525	2.82	0.82
	WAT	2.89	0.73	ETA	2.92	0.84
	WAT	2.83	0.76	ETA	2.73	0.79

Table 2. Average hydrogen bond distance and fraction of hydrogen bond lifetime for high affinity binding sites.

three hydrogen bonds (Tyr 411, Arg 410 of HSA and one molecule of water) in **site 4**. However, in the solvent mixture, the stearic acid molecule in **site 4** is only able to establish two conserved hydrogen bonds with Tyr 411 and Ser 489 of HSA. The 3-D representation of the three high affinity fatty acid binding sites (**site 1**, **site 2**, **site 5**) in both systems (water and 20 % ethanol-water) also evidence the role of solvent interactions on the stabilisation of specific binding motifs (Fig. 4).

Next, we compare representative snapshots from the MD simulations of the stearic acid-albumin complex (with stearic acid in **site 1**) under different solvent conditions with the reported crystal structure of stearic acid-albumin (PBD ID: 1E7I) (Fig. 5). The comparison indicates that the stearic acid molecule adopts a less compact conformation in the 20 % ethanol-water mixture with respect to the control system (water). A higher conformational flexibility of the stearic acid molecule in the solvent mixture may enable it to establish more hydrogen bond contacts with strong affinity.

Overall, we observed that the solvent has modulating effects on the binding of the fatty acid to a particular site of human serum albumin. **Site 1**, which was amongst the low affinity fatty acid binding sites in water, emerged as a high affinity-binding site in the ethanol-water mixture.

4 Conclusions

Here we show that altering solvent composition can be a useful tool for modulating biomolecular function, in this case the binding specificity of human serum albumin as a carrier of fatty acids. Low affinity to high affinity fatty acid binding site conversion was achieved when using, instead of water as solvent, a 20 % water-ethanol mixture. Conversely, a high affinity fatty acid binding site transitioned to low affinity under the same conditions. Our findings, which we rationalise at the molecular level, have special relevance for the regulation of biological function since we show that the targeted manipula-

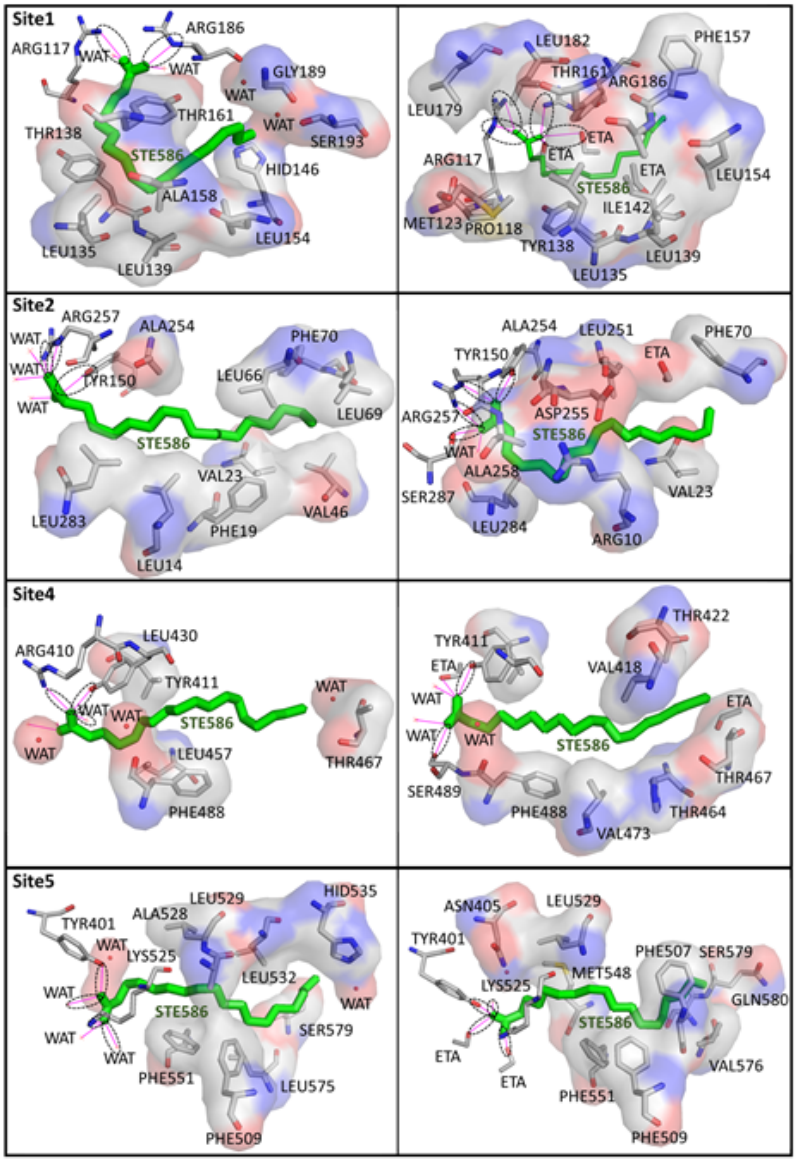

Figure 4. Structure of HSA in water (left panel) and in 20 % ethanol-water for **site 1**, **site 2, site 4** and **site 5**. Residues/molecules involved in van der Waals interactions are shown in surface representation (vdW colour cloud with red for oxygen, blue: nitrogen, gray: carbon). The stearic acid molecule is shown in green sticks. Conserved hydrogen bond contacts are circled.

tion of protein-ligand binding events can be achieved by rationally tuned solvent-driven interactions.

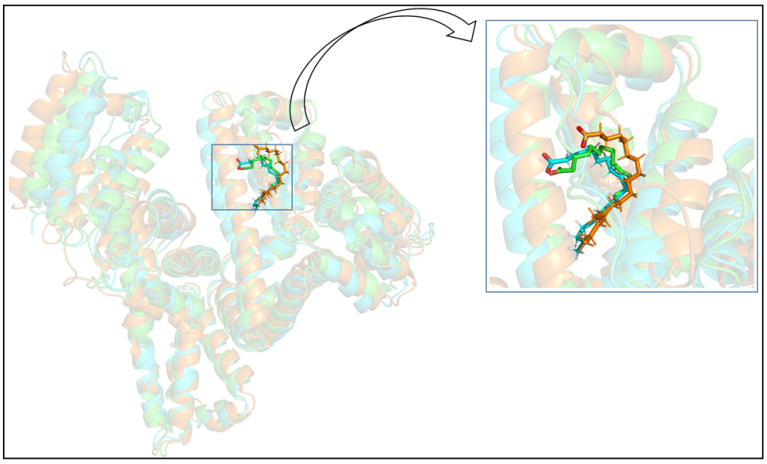

Figure 5. Overlay of the structures of human serum albumin in the crystal structure (green), in water (cyan) and in the 20 % ethanol-water mixture (orange) with stearic acid bound to **site 1** (close-up as inset). Water and counterions were removed for clarity.

Acknowledgements

This work was supported by the Deutsche Forschungsgemeinschaft (DFG, German Research Foundation) under Germany's Excellence Strategy – EXC-2033 – Projektnummer 390677874 and by the FP-RESOMUS program. E. S.-G. also acknowledges the support of the Boehringer Ingelheim Foundation (Plus-3 Program). Y. R.-B and E. S.-G. gratefully acknowledge the computing time granted by the John von Neumann Institute for Computing (NIC) and provided on the supercomputer JURECA at Jülich Supercomputing Centre (JSC). E. S.-G. acknowledges the working group Albunet for Albumin studies and Dr. Katja Waterstradt for experimental collaboration.

References

1. S.-I. Fujiwara, T. Amisak *et al.*, *Identification of High Affinity Fatty Acid Binding Sites on Human SerumAlbumin by MM-PBSA Method*, Biophys. J. **94**, 95–105, 2008.
2. Q. Qian, Z. You, L. Ye, J. Che, Y. Wang, S. Wang, and B. Zhong, *High-efficiency production of human serum albumin in the posterior silk glands of transgenic silkworms, Bombyx mori L*, PLoS ONE **13**, e0191507, 2018.
3. C. Cai, K. Zhou, Y. Wu, and L. Wu, *Enhanced liver targeting of 5-fluorouracil using galactosylated human serum albumin as a carrier molecule*, J. Drug Targ. **14**, 55–61, 2006.
4. A. Lamousé-Smith, G. M. Subramanian, M. Fiscella, S. Zeuzem, and J. G. McHutchison, *Albinterferon alpha-2b: a genetic fusion protein for the treatment of chronic hepatitis C*, Nat. Biotech. **25**, 1411–1419, 2007.
5. D. Bratlid and T. Bergan, *Displacement of albumin-bound antimicrobial agents by bilirubin*, Pharmacology **14**, 464–472, 1976.

6. A. Dalhoff, *Seventy-Five Years of Research on Protein Binding*, Antimicrob Agents Chemother **62**, e01663-17, 2018.
7. S. Yuge, M. Akiyama, and T. Komatsu, *An Escherichia coli trap in human serum albumin microtubes*, Chem. Commun. **50**, 9640–9643, 2014.
8. U. Kragh-Hansen, *Molecular aspects of ligand binding to serum albumin*, Pharmacol. ReV. **33**, 17–53, 1981.
9. J. Seetharamappa and B. J. Kamat, *Study of the interaction between fluoroquinolones and bovine serum albumin*, J. Pharm. Biomed. **39**, 1046–1050, 2005.
10. S. Curry, P. Brick, and N. P. Franks, *Fatty acid binding to human serum albumin: new insights from crystallographic studies*, Biochim. Biophys. Acta **1441**, 131–140, 1999.
11. P. M. Wiggins, *Role of water in some biological processes*, Microbiol Rev. **54**, 432–449, 1990.
12. D. Roccatano, *Computer simulations study of biomolecules in non-aqueous or cosolvent/water mixture solutions*, Current Protein & Peptide Science **9**, 407–426, 2008.
13. L. Yang, J. S. Dordick, and S. Garde, *ydration of enzyme in nonaqueous media is consistent with solvent dependence of its activity*, Biophys. J. **87**, 812–821, 2004.
14. S. K. Pal and A. H. Zewail, *Dynamics of Water in Biological Recognition*, Chem. Rev. **104**, 2099–2123, 2004.
15. G. A. Papoian, J. Ulander, and P. G. Wolynes, *Role of Water Mediated Interactions in ProteinProtein Recognition Landscapes*, J. Am. Chem. Soc. **125**, 9170–9178, 2003.
16. B. Jayaram and T. Jain, *The role of water in Protein-DNA recognition*, Ann. Rev. Biophy. Biomol. Struc. **33**, 343–361, 2004.
17. S. Wong, R. E. Amaro, and J. A. McCammon, *MM-PBSA Captures Key Role of Intercalating Water Molecules at a ProteinProtein Interface*, J. Chem. Theory Comput. **5**, 422–429, 2009.
18. D. Russo, G. Hura, and T. Head-Gordon, *Hydration Dynamics Near a Model Protein Surface* Biophys. J. **86**, 1852–1862, 2004.
19. P. Ball, *Water as an active constituent in cell biology*, Chem. Rev. **108**, 74–108, 2008.
20. Y. Yu, J. Wang, Q. Shao, J. Shi, and W. Zhu, *The effects of organic solvents on the folding pathway and associated thermodynamics of proteins: a microscopic view*, Sci. Rep. **6**, 19500, 2016.
21. G. Carrea and S. Riva, *Properties and Synthetic Applications of Enzymes in Organic Solvents*, Angew. Chem. Int. Ed. **39**, 2226–2254, 2000.
22. S. E. Graham, N. Leja, and H. A. Carlson, *MixMD Probeview: Robust Binding Site Prediction from Cosolvent Simulations*, J. Chem. Inf. Model. **58**, 1426–1433, 2018.
23. P. Lee and X. Wu, *Review: modifications of human serum albumin and their binding effect*, Curr. Pharm. Des. **21**, 1862–1865, 2015.
24. J. R. Simard, P. A. Zunszain, C.-E. Ha, J. S. Yang, N. V. Bhagavan, I. Petitpas, S. Curry, and J. A. Hamilton, *Locating high-affinity fatty acid-binding sites on albumin by x-ray crystallography and NMR spectroscopy*, Proc. Natl. Acad. Sci. USA **102**, 17958–17963, 2005.
25. D. S. Goodman, and E. Shafrir, *The Interaction of Human Low Density Lipoproteins with Long-chain Fatty AcidAnions*, J. Am. Chem. Soc. **81**, 364–370, 1959.
26. H. Gohlke, and D. A. Case, *onverging free energy estimates: MM-PB(GB)SA studies on the protein protein complex Ras-Raf*, J. Comput. Chem. **25**, 238–250, 2004.

27. H. M. Berman, J. Westbrook, Z. Feng, G. Gilliland, T. N. Bhat, H. Weissig, I. N. Shindyalov, and P. E. Bourne, *The Protein Data Bank*, Nucleic Acids Res. **28**, 235–242, 2000.
28. J. Yang and Y. Zhang, *I-TASSER server: new development for protein structure and function predictions*, Nucleic Acids Res. **43**, W174–W181, 2015.
29. A. Sivertsen, J. Isaksson, H.-K. S. Leiros, J. Svenson, J.-S. Svendsen, and B.-O. Brandsdal, *Synthetic Cationic Antimicrobial Peptides Bind with Their Hydrophobic Parts to Drug Site II of Human Serum Albumin*, Bmc Struc. Biol. **14**, 4–13, 2014.
30. R. Anandakrishnan, B. Aguilar, and A. O. Onufriev, *H++ 3.0: automating pK prediction and the preparation of biomolecular structures for atomistic molecular modeling and simulations*, Nucleic Acids Res. **40**, W537–541, 2012.
31. D. A. Case *et al.*, *AMBER 14*, University of California, San Francisco, 2014.
32. J. A. Maier, C. Martinez, K. Kasavajhala, L. Wickstrom, K. Hauser, and C. Simmerling, *ff14SB: Improving the Accuracy of Protein Side Chain and Backbone Parameters from ff99SB*, J. Chem. Theory Comput. **11**, 3696–3713, 2015.
33. J. C. Phillips, R. Braun, W. Wang, J. Gumbart, E. Tajkhorshid, E. Villa, C. Chipot, R. D. Skeel, L. Kalé, K. Schulten, *Scalable molecular dynamics with NAMD*, J. Comput. Chem. **26**, 1781–1802, 2005.
34. J. Huang, S. Rauscher, G. Nawrocki, T. Ran, M. Feig, B.-L. de Groot, H. Grubmüller, and M. A. MacKerell Jr., *CHARMM36m: an improved force field for folded and intrinsically disordered proteins*, Nat. Methods. **14**, 71–73, 2017.
35. K. Vanommeslaeghe, E. Hatcher, C. Acharya, S. Kundu, S. Zhong, J. Shim, E. Darian, O. Guvench, P. Lopes, I. Vorobyov, and A. D. MacKerell Jr., *CHARMM general force field: A force field for drug-like molecules compatible with the CHARMM all-atom additive biological force fields*, J. Comput. Chem. **31**, 671–690, 2009.
36. E. Vanquelef, S. Simon, G. Marquant, E. Garcia, G. Klimerak, J. C. Delepine, P. Cieplak, and F. Y. Dupradeau, *R.E.D. Server: a web service for deriving RESP and ESP charges and building force field libraries for new molecules and molecular fragments*, Nucleic Acids Res. **39**, W511–W517, 2011.
37. W. D. Cornell *et al.*, *A Second Generation Force Field for the Simulation of Proteins, Nucleic Acids and Organic Molecules*, J. Am. Chem. Soc. **117**, 5179–5197, 1995.
38. T. E. Cheatham III, J. L. Miller, T. Fox, T. A. Darden, and P. A. Kollman, *Molecular Dynamics Simulations on Solvated Bio-molecular Systems: The Particle Mesh Ewald Method Leads to Stable Trajectories of DNA, RNA and Proteins*, J. Am. Chem. Soc. **117**, 4193–4194, 1995.
39. D. R. Roe and T. E. Cheatham III, *PTRAJ and CPPTRAJ: Software for Processing and Analysis of Molecular Dynamics Trajectory Data*, J. Chem. Theory Comput. **9**, 3084–3095, 2013.
40. L. Martínez, R. Andrade, E. G. Birgin, and J. M. Martínez, *PACKMOL: a package for building initial configurations for molecular dynamics simulations*, J. Comput. Chem. **30**, 2157–2164, 2009.
41. W. Humphrey, A. Dalke, and K. Schulten, *VMD: visual molecular dynamics*, J. Molec. Graphics **14**, 33–38, 1996.
42. R. A. Laskowski and M. B. Swindells, *LigPlot+: multiple ligand-protein interaction diagrams for drug discovery*, J. Chem. Inf. Model. **51**, 2778–2786, 2011.